**Structural Monitoring and Maintenance**, *Vol. 1, No. 2 (2014) 213-230*
DOI: http://dx.doi.org/10.12989/smm.2014.1.2.213 

# Actuator and sensor failure detection using direct approach

Zhiling Li and Satish Nagarajaiah*

*Department of civil and environmental engineering, Rice University, Houston, TX, USA, 77005*

*(Received March 15, 2014, Revised May 25, 2014, Accepted June 7, 2014)*

**Abstract.** A novel real-time actuator failure detection algorithm is developed in this paper. Actuator fails when the input to the structure is different from the commanded one. Previous research has shown that one error function can be formulated for each actuator through interaction matrix method. For output without noise, non-zero values in the actuator functions indicate the instant failure of the actuator regardless the working status of other actuators. In this paper, it is further demonstrated that the actuator's error function coefficients will be directly calculated from the healthy input of the examined actuator and all outputs. Hence, the need for structural information is no longer needed. This approach is termed as direct method. Experimental results from a NASA eight bay truss show the successful application of the direct method for isolating and identifying the real-time actuator failure. Further, it is shown that the developed method can be used for real-time sensor failure detection.

**Keywords:** actuator failure; sensor failure; direct method; interaction matrix method

## 1. Introduction

Control systems have been widely used in civil engineering, especially in Japan (Spencer and Nagarajaiah 2003). The performance of the structures with control systems depends on the actuators and sensors. Hence, damaged actuators/sensors shall be real-time identified and isolated to ensure the safety of the host structure.

An actuator fails when its input to the structure is different from the commanded one. With multiple actuators, structural responses are all influenced even only some actuators fail. Simply comparing structural responses cannot distinguish the failed actuators. To identify the failed actuators, an indication function is needed for each actuator and the influence of all other actuators on this indication function shall be eliminated.

Various actuator failure detection and isolation techniques have been discussed over the past decades (Frank 1990, Gertler 1991, Chen and Patton 1999). Most of them utilize the model based Analytical Redundancy (AR) contained in the static and dynamic relationship among the system inputs and measured outputs (Frank 1990). The first well-developed actuator detection algorithm using AR method was developed by Beard (1971) and restudied by Jones (1973), which was termed as Beard-Jones Detection filter(BJDT). The BJDT was designed by assigning fixed directional properties to the error function through observer design method. Non-zero values in the error function indicate the real-time failure of the examined actuator without output noise.

*Corresponding author, Professor, E-mail: satish.nagarajaiah@rice.edu


http://www.techno-press.org/?journal=smm&subpage=7 ISSN: 2288-6605 (Print), 2288-6613 (Online)

Massoumnia (1986) used geometric approach to restudy BJDT. White and Speyer (1987) applied eigen assignment technique to calculate the detection filter gain and the close-loop eigenvectors. The eigen assignment technique for fault detection was extendedly studied in Patton's group (Chen and Patton 1999). Another observer based method, the Unknown Input Observer (UIO) method, which was originally proposed by Watanabe and Himmelblau (1982), used a set of observers such that each observer is chosen to make the unknown input unobservable to the residual. The UIO was first proposed to make the state-estimation error decouple from the unknown input (disturbance) and was extended by Wunnenberg (1990), Wunnenberg and Frank (1987) to isolate the sensor and actuator failure.

In discrete domain, parity based detection filters have been extensively studied by many researchers (Mironovski 1979, 1980, Chow and Willsky 1984, Gertler *et al*. 1990, Gertler and Dipierro 1997, Gertler 1998). Gertler (1991) has proven that the parity and observer-based method are equivalent.

Via interaction matrix method, previous study (Koh *et al*. 2005) has shown that an error function is built for each actuator using only the commanded input from the examined actuator and all measured outputs. Without measurement noise, the error function will be non-zero when the examined actuator fails. The error function coefficients are calculated from the discrete state space matrices A, B, C, and D, which can be identified from the healthy input-output data using system realization methods, such as Observer/Kalman filter IDentification (OKID) and Eigen system Realization Algorithm (ERA). Hence, the error during system identification is brought into the error function. As discussed previously (Koh *et al*. 2005), to get good error functions, the number of identified states using OKID-ERA method have to be increased to match the simulated outputs with the real output, especially when output noise exists.

In this study, an approach is designed to calculate each actuator's error function coefficient directly from the healthy input of the examined actuator and all measured outputs. Thus the need for the structural state-space model is bypassed and the error incurred during system realization is avoided. This approach is termed as direct method in this paper. Using the same idea, we further demonstrate that the direct method can be used for real-time sensor failure detection and isolation without knowing the inputs information.

## 2. Review of the indirect method

As shown in previous paper (Koh *et al*. 2005), by introducing the interaction matrix, a bunch of error functions are formed, one for each actuator. Each error function, using only the commanded input from the examined actuator and all measured outputs, can monitor the working status of the examined actuator regardless the condition of other actuators. The existence condition of interaction matrix allows eliminating the dependence of all other inputs except the examined one from the corresponding error function. In this section, the procedure of the actuator failure using interaction matrix method, which will form the theoretic basis for the direct approach, will be briefly discussed first.

Consider an $n$-th order, $r$-input, $q$-output linear time-invariant discrete state space model

$$\begin{aligned} x(k+1) &= \mathbf{A}x(k) + \mathbf{B}u(k) \\ y(k) &= \mathbf{C}x(k) + \mathbf{D}u(k) \end{aligned} \tag{1}$$

By repeating and substituting the equations in Eq. (1) for $p>0$ steps and regrouping the inputs from each actuator as one term gives

$$\begin{aligned} x(k+1) &= \mathbf{A}^p x(k) + \sum_{j=1}^{r} \Gamma_j u_{pj}(k) \\ y_p(k) &= \mathbf{O}x(k) + \sum_{j=1}^{r} \mathbf{T}_j u_{pj}(k) \end{aligned} \tag{2}$$

Where $\Gamma_j$ is the extended $n \times p$ controllability matrix for the $j$-th input, O is the extended $pq \times n$ observability matrix, and $\mathrm{T}_j$ is an $pq \times p$ 'Toeplitz' matrix of the system Markovara meters of the $j$-th input, $\mathrm{u}_{pj}(k)$ and $\mathrm{y}_p(k)$ are column vectors of the $j$-th input and output data going $p$ steps into future starting with $u_j$ and $\mathrm{y}(k)$, respectively

$$\Gamma_j = \left[ \mathbf{A}^{p-1}\mathbf{B}_j \ \mathbf{A}^{p-2}\mathbf{B}_j \ \cdots \ \mathbf{B}_j \right],$$

$$\mathbf{O} = \begin{bmatrix} \mathbf{D}_j \\ \mathbf{CA} \\ \vdots \\ \mathbf{CA}^{p-1} \end{bmatrix}, \quad \mathbf{T}_j = \begin{bmatrix} \mathbf{D}_j & \mathbf{0} & \cdots & \mathbf{0} \\ \mathbf{CB}_j & \mathbf{D}_j & \cdots & \mathbf{0} \\ \mathbf{CAB}_j & \mathbf{CB}_j & \cdots & \mathbf{0} \\ \vdots & \vdots & \ddots & \vdots \\ \mathbf{CA}^{p-2}\mathbf{B}_j & \mathbf{CA}^{p-2}\mathbf{B}_j & \cdots & \mathbf{D}_j \end{bmatrix},$$

$$\mathbf{u}_{pj}(k) = \begin{pmatrix} \mathbf{u}_j(k) \\ \mathbf{u}_j(k+1) \\ \vdots \\ \mathbf{u}_j(k+p-1) \end{pmatrix}, \quad \mathbf{y}_p(k) = \begin{pmatrix} \mathbf{y}(k) \\ \mathbf{y}(k+1) \\ \vdots \\ \mathbf{y}(k+p-1) \end{pmatrix}.$$

An interaction matrix $\mathrm{M}_i$ is introduced by adding and subtracting the product $\mathrm{M}_i \mathrm{y}_p(k)$ into the state equation in Eq. (2). The output equation at $k$+$p$ step in Eq. (2) is rewritten below by substituting the state equation into it.

$$\mathbf{y}(k+p) = (\mathbf{CA}^P + \mathbf{CM}_i\mathbf{O})\mathbf{x}(k) + \sum_{j=1}^{r}(\mathbf{C\Gamma}_j + \mathbf{CM}_i\mathbf{T}_j)\mathbf{u}_{pj}(k) - \mathbf{CM}_i\mathbf{y}_p(k) + \sum_{j=1}^{r}\mathbf{D}_j\mathbf{u}_j(k+p) \tag{3}$$

To build an input-output relationship for examined actuator and all outputs, the coefficient matrix before initial condition $\mathrm{x}(k)$ and the coefficient matrices before all inputs except the examined $i$-th actuator shall be eliminated, which is done by imposing the conditions for product $\mathrm{CM}_i$ and $\mathrm{N}_i^T$ in Eq. (4)

$$\begin{aligned} &\mathbf{CA}^{p} + \mathbf{CM}_i\mathbf{O} = 0 \\ &\mathbf{C\Gamma}_j + \mathbf{CM}_i\mathbf{T}_j = 0 \quad \textit{for} \;\; j \neq i \\ &\mathbf{N}_i^T\mathbf{D}_j \neq 0 \qquad\qquad \textit{for} \;\; j \neq i \end{aligned} \tag{4}$$

By multiplying the row vector $\mathrm{N}_i^T$ on both size of Eq. (3) and adding the constraint conditions

In Eq. (4)

$$\mathbf{N}_i^T\mathbf{y}(k+p) = \mathbf{N}_i^T(\mathbf{C\Gamma}_i + \mathbf{CM}_i\mathbf{T}_i)\mathbf{u}_{pi}(k) - \mathbf{N}_i^T\mathbf{CM}_i\mathbf{y}_p(k) + \mathbf{N}_i^T\mathbf{D}_i\mathbf{u}_i(k+p) \tag{5}$$

To derive an actuator failure detection equation, the actuator input $\mathrm{u}_i(k)$ is replaced by a summation of commanded input $\bar{\mathrm{u}}_i(k)$ (known) and actuator error $\mathrm{u}_i^*(k)$ (unknown). Eq. (4) is rewritten as

$$\begin{aligned} &\mathbf{N}_i^T\mathbf{y}(k+p) = \mathbf{N}_i^T(\mathbf{C\Gamma}_i + \mathbf{CM}_i\mathbf{T}_i)(\bar{u}_{pi}(k) + u_{pj}^*(k)) - \mathbf{N}_i^T\mathbf{CM}_i\mathbf{y}_p(k) \\ &+ \mathbf{N}_i^T\mathbf{D}_i(\bar{u}_{pi}(k+p) + u_{pj}^*(k+p)) \end{aligned} \tag{6}$$

Defining the *i*-th actuator's error function as

$$e_i(k+p) = \mathbf{N}_i^T(\mathbf{C\Gamma}_i + \mathbf{CM}_i\mathbf{T}_i)u_{pi}^*(k) + \mathbf{N}_i^T\mathbf{D}_i u_i^*(k+p) \tag{7}$$

And the actuator error function is calculated by

$$e_i(k+p) = \mathbf{N}_i^T\mathbf{CM}_i\mathbf{y}_p(k) + \mathbf{N}_i^T\mathbf{y}(k+p) - \mathbf{N}_i^T(\mathbf{C\Gamma}_i + \mathbf{CM}_i\mathbf{T}_i)\bar{u}_{pj}(k) - \mathbf{N}_i^T\mathbf{D}_i\bar{u}_i(k+p) \tag{8}$$

To isolate the *i*-th input from other inputs in the error function, the number of independent measurements shall be equal to or greater than the number of inputs and also the integer $p$ shall be greater than or equal to $n/(q-r+1)$, as discussed in the previous paper (Koh *et al.* 2005).

When the number of independent measurements is greater than or equal to the number of inputs, an error function for each actuator is developed via the interaction matrix formulation. This error function can monitor the real-time failure of the examined actuator. The error function has the general form

$$e_i(k) = \alpha_0^i\mathbf{y}(k) + \alpha_1^i\mathbf{y}(k-1) + \cdots + \alpha_p^i\mathbf{y}(k-p) + \beta_0^i\bar{u}_i(k) + \beta_1^i\bar{u}_i(k-1) + \cdots + \beta_p^i\bar{u}_i(k-p) \tag{9}$$

Where $\bar{\mathrm{u}}_i(k)$ is the commanded input to the *i*-th actuator, and integer $p$ must be greater than or equal to $n/(q-r+1)$. For an $r$-input and $q$-output system ( $q \geq r$ ), each coefficient of $\alpha_0^i,\ \alpha_1^i,\ \cdots,\ \alpha_p^i$ is a $1\times q$ row vector and each coefficient of $\beta_0^i,\ \beta_1^i,\ \cdots,\ \beta_p^i$ is a scalar. When the *i*-th actuator does not fail, $e_i(k) = 0$.

Each error function's coefficients are calculated from the state space model and the state space matrices can be identified from the input-output data using system identification methods. Since the actuator error functions are calculated from the state-space model, this approach is termed as indirect method in this paper.

The main steps using indirect method are summarizes as

1. Identified the system state-space matrices **A**, **B**, **C**, and **D** from healthy input-output data using system realization method, such as OKID-ERA.
2. For each actuator, solve $CM_i$ and $N_i$ using Eq. (4).
3. Calculate the coefficients of the error function for the *i*-th actuator in Eq. (8) using the computed $CM_i$ and $N_i$.
4. Compute the error function using *i*-th commanded input and all measured structural responses by Eq. (9).
5. Repeat steps 1 ~ 4 to obtain the error function coefficients for each actuator.
6. Monitor the actuator's working status using the error function.

## 3. Mathematical formulation for direct method

The structure and existence condition for the actuator error function have been discussed in last section. This section will focus how to calculate the error function's coefficients directly from the healthy input-output data without state space matrices. Hence, the need to know the state-space model is bypassed. This approach is termed as direct method in this paper. This strategy turn out to be particularly advantageously in practice because it bypasses the intermediate system realization step and avoids the error incurred during such realization.

When the examined *i*-th actuator works functionally, the error function equals to zero

$$\alpha_0^i \mathbf{y}(k) + \alpha_1^i \mathbf{y}(k-1) + \cdots + \alpha_p^i \mathbf{y}(k-p) + \beta_0^i \bar{u}_i(k) + \beta_1^i \bar{u}_i(k-1) + \cdots + \beta_p^i \bar{u}_i(k-p) = 0 \quad (10)$$

### *3.1 Direct method 1*

When the *i*-th actuator works, the right hand side of Eq. (10) is zero. The error function coefficients are not fixed unless they are 'normalized' in some way, say for example by keeping the value of $\beta_p^i$ being minus one. By doing so, Eq. (10) is rewritten as

$$\begin{aligned} \bar{u}_p(k-p) = \alpha_0^i \mathbf{y}(k) + \alpha_1^i \mathbf{y}(k-1) + \cdots + \alpha_p^i \mathbf{y}(k-p) + \beta_0^i \bar{u}_i(k) + \beta_1^i \bar{u}_i(k-1) \\ + \cdots + \beta_{p-1}^i \bar{u}_i(k-p+1) \end{aligned} \quad (11)$$

From a set of sufficient rich and long input-output data

$$\{\bar{u}_i(k-p), \bar{u}_i(k-p+1), \cdots, \bar{u}_i(k-p+l)\}, \ \{y(k), y(k+1), \cdots, y(k+l)\} \quad (12)$$

Eq. (11) can be written as

$$\mathbf{U}_i = \mathbf{P}_i \mathbf{V}_i \quad (13)$$

where

$$\mathbf{U}_i = \{\bar{u}_i(k-p), \bar{u}_i(k-p+1), \cdots, \bar{u}_i(k-p+l)\}$$
$$\mathbf{P}_i = \{\ \beta_0\ \cdots\ \beta_{p-1}\ \ \alpha_0\ \cdots\ \alpha_{p-1}\ \ \alpha_p\ \} \tag{14}$$
$$\mathbf{V}_i = \begin{pmatrix} \bar{u}_i(k) & \bar{u}_i(k+1) & \cdots & \bar{u}_i(k+l) \\ \vdots & \vdots & \ddots & \vdots \\ \bar{u}_i(k-p) & \bar{u}_i(k-p+1) & \cdots & \bar{u}_i(k-p+l+1) \\ y(k) & y(k+1) & \cdots & y(k+l) \\ \vdots & \vdots & \ddots & \vdots \\ y(k-p) & y(k+1-p) & \cdots & y(k+l-p) \end{pmatrix}$$

Thus the *i*-th error function's coefficients are calculated through matrix pseudo inverse

$$\mathbf{P}_i = \mathbf{U}_i\left(\mathbf{V}_i\right)^+ = \mathbf{U}_i\mathbf{V}_i^T\left(\mathbf{V}_i\mathbf{V}_i^T\right)^+ \tag{15}$$

where the $()^+$ sign denotes the pseudo-inverse, which shall be computed via singular value decomposition method.

### 3.2 Direct method 2

Another way to calculate the error function's coefficients or the examined *i*-th actuator from the input-output data will also be discussed here. The input from the examined *i*-th actuator and all measured structural responses satisfy the input-output relationship in Eq. (10). By rewriting Eq. (10) as

$$\bar{\mathbf{P}}_i\bar{\mathbf{V}}_{ik} = 0 \tag{16}$$

Where

$$\bar{\mathbf{P}}_i = \{\ \beta_0^i\ \cdots\ \beta_{p-1}^i\ \ \beta_p^i\ \ \alpha_0^i\ \cdots\ \alpha_{p-1}^i\ \ \alpha_p^i\ \}$$
$$\bar{\mathbf{V}}_{ik} = \begin{pmatrix} \bar{u}_i(k) \\ \bar{u}_i(k-1) \\ \vdots \\ \bar{u}_i(k-p) \\ \bar{y}_i(k) \\ \bar{y}_i(k-1) \\ \vdots \\ \bar{y}_i(k-p) \end{pmatrix} \tag{17}$$

Expressing Eq. (17) for *l*-steps

$$\bar{\mathbf{P}}_i \bar{\mathbf{V}}_{ik}^l = 0 \tag{18}$$

Where

$$\bar{\mathbf{V}}_{ik}^l = \begin{bmatrix} \bar{\mathbf{V}}_{ik} & \bar{\mathbf{V}}_{i(k+1)} & \cdots & \bar{\mathbf{V}}_{i(k+l)} \end{bmatrix} \tag{19}$$

In order for Eq. (18) to be satisfied, the row vector $\bar{\mathrm{P}}_i$ must belong to the left null-space of the matrix $\bar{\mathrm{V}}_{ik}^l$, which is calculated by applying singular value decomposition (SVD) method on matrix $\bar{\mathrm{V}}_{ik}^l$

$$\bar{\mathbf{V}}_{ik}^l = \begin{bmatrix} \mathbf{U}_{1i}, & \mathbf{U}_{2i} \end{bmatrix} \begin{bmatrix} \mathbf{S}_{1i} & 0 \\ 0 & 0 \end{bmatrix} \begin{bmatrix} \mathbf{V}_{1i}^T \\ \mathbf{V}_{2i}^T \end{bmatrix} \tag{20}$$

From Eq. (20), any row vector or linear combination of the row vectors in $\mathrm{U}_{2i}^T$ can be taken as $\bar{\mathrm{P}}_i$ .Hence, $\bar{\mathrm{P}}_i$ is not unique. To make the function robust to measured noise, row vector $\bar{\mathrm{P}}_i$ shall be as orthogonal as possible to the sensor noise direction. If assuming the noise levels at all sensors are the same, the sensor noise directions are expressed as

$$\bar{\mathbf{N}}_i = \begin{bmatrix} \mathbf{0} & \mathbf{0} & \cdots & \mathbf{0} \\ \mathbf{0} & \mathbf{0} & \cdots & \mathbf{0} \\ \mathbf{0} & \mathbf{0} & \cdots & \mathbf{0} \\ \mathbf{0} & \mathbf{0} & \cdots & \mathbf{0} \\ \mathbf{I} & \mathbf{0} & \cdots & \mathbf{0} \\ \mathbf{0} & \mathbf{I} & \cdots & \mathbf{0} \\ \vdots & \vdots & \ddots & \vdots \\ \mathbf{0} & \mathbf{0} & \cdots & \mathbf{I} \end{bmatrix} \tag{21}$$

To minimize the sensor noise influence to the error function, $\mathrm{P}_i$ should: 1) belong to the row vector or linear combination of the row vector in $\mathrm{U}_{2i}^T$, and 2) be as orthogonal as possible to $\mathrm{N}_i$ . This problem is formed as the following equations

$$\mathrm{P}_i = \sum_j \left(\lambda_j^i \mathrm{U}_{2i}(:,j)\right)^T \tag{22}$$

$$\min(\bar{\mathrm{N}}_i \bar{\mathrm{P}}_i^T) = \left[ \bar{\mathrm{N}}_i U_{2i} \begin{pmatrix} \lambda_1^i \\ \vdots \\ \lambda_s^i \end{pmatrix} \right]$$

Again applying SVD on $\bar{\mathrm{N}}_i \mathrm{U}_{2i}$

$$\bar{\mathrm{N}}_i \mathrm{U}_{2i} = \tilde{\mathrm{U}}_i \tilde{\mathrm{S}}_i \tilde{\mathrm{V}}_i^T \tag{23}$$

and $[\lambda_1^i, \cdots, \lambda_s^i]$ can be taken as transpose of the last row vector in $\tilde{V}_i$.

The main steps in the direct methods can be summarized as

1. For direct method 1, calculate *i*-th actuator's error function's coefficients from the healthy input/output data from Eq. (14); for direct method 2, calculate the error function's coefficients from the healthy input-output data using Eqs. (20) and (23).
2. Monitor the actuator's working status using the error function computing from *i*-th commanded input and all measured structural responses by Eq. (9).
3. Repeat steps 1 ~ 2 for each actuator.

## 4. Applied for sensor failure detection

In this section, it is further shown the direct methods can also be used for sensor failure detection with output measurement only. Sensor failure considered in this paper can be any type of measurement error that is different from the true structural response. To detect sensor failure, sensors are separated into two groups. Sensors in the first group are assumed to correctly measure the structural responses and are termed as reference sensors in this paper. Sensors in the second group to be monitored are termed as uncertain sensors. A sensor error function, one for each uncertain sensor, is developed to monitor the real-time failure of the uncertain sensor. Non-zero values in the sensor error function indicate the real-time failure of the examined uncertain sensor and it is not influenced by other uncertain sensors. Indirect sensor failure approach has been discussed in another paper (Li *et al*. 2007) and it forms the theoretical basis for direct sensor failure detection method. The basic steps to formulate indirect sensor failure detection methods are: 1) using inverse model to eliminate inputs from the state space matrices, 2) applying interaction matrix to build the relationship between examined uncertain sensor and all reference sensors. Brief description can be found in referred paper (Li *et al*. 2007).

The *i*-th uncertain sensor's error function has the following general form

$$\begin{aligned} e_i(k) = \alpha_0^i y_s(k) + \alpha_1^i y_s(k-1) + \cdots + \alpha_p^i y_s(k-p) \\ + \beta_1^i \bar{y}_d^i(k-1) + \cdots + \beta_p^i \bar{y}_d^i(k-p) \end{aligned} \tag{24}$$

where $y_s(k)$ is the measured outputs from all reference sensors at *k*-th step and $y_d^i(k)$ is the measured output from the *i*-th uncertain sensor at *k*-th step. $\alpha_i$ and $\beta_i$ are the sensor error function coefficients. If the *i*-th uncertain sensor works and all reference sensors' measured noises are zeros, the error function is zero. Using the method discussed in last section, each uncertain sensor's error function can be calculated.

## 5. Experimental verification

### 5.1 Experimental verification for direct actuator failure detection method

This section discusses the experimental verification for actuator failure using direct methods and compares the results between the direct methods and indirect methods.

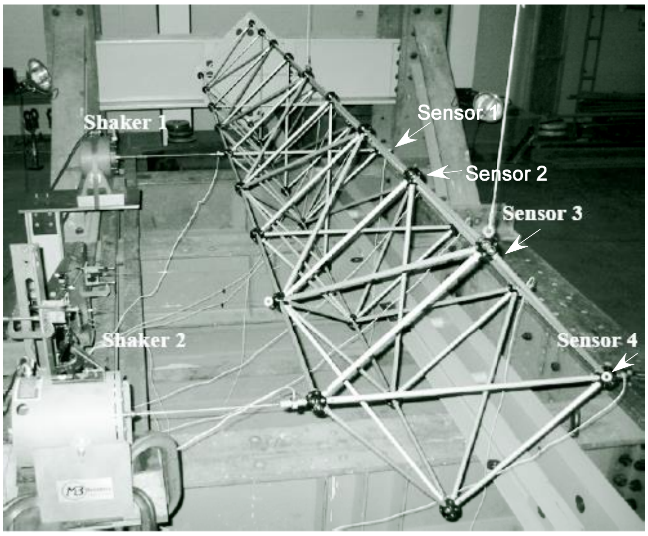


Fig. 1 Picture of an Eight Bay Truss Structure

The test bed is a 4.0 meter long eight bays truss, which is a part structure of a NASA space station. The test truss is composed with 109 aluminum members and 32 node balls. The hollow aluminum members, with 0.5 inches outer diameter and 0.1 inches thickness, fit with bolt ends which can be screwed into the node balls. One end of the truss is fixed to a steel frame and the steel frame is fixed to the ground, as shown in Fig. 1.

Two shakers are connected to the truss: one at the first bay and the other at the fifth bay of the truss, counted from the free end of the truss and hence forth. Bending flexible stinger rods are used to connect the shakers to the nodes in the corresponding bays. The stingers transmit the input force in the axial direction and are flexible in other directions. Load cells are installed between the stingers and the nodes of the corresponding bays to measure the actuator input force. In this experiment, two hangers are connected to the truss nodes at the first and fifth bays to constraint vertical movement, as shown in Fig. 1. So only lateral movement is considered in this study. To isolate the input failure from the two shakers, at least two sensors are needed. In this study, two accelerometers are mounted to the nodes at the first and forth bays of the truss.

In this experiment, two shakers are driven by independent banded-limited white noise signals from two amplifiers, controller by the dSPACE board built in a personal computer. Load cells and accelerometers are first connected to PCB 481A signal conditioner and then connected to the same dSPACE board. The sampling time is 0.001 seconds and total simulation time is 50 seconds. For direct methods, the coefficients of the error function for each shaker are calculated from the healthy input-output data. For indirect method, the state-space matrices **A**, **B**, **C**, and **D** are first calculated from the healthy input-output data using OKID-ERA method and then the coefficients of the error functions are calculated from the realized state-space matrices by following the steps summarized in Section 2. To generate actuator failure, shaker one was turn off during 20~40 seconds and shaker 2 was turn off during 10~15 and 30~40seconds.

To compare the results, the error functions for the two shakers generated by indirect method, direct method 1, and direct method 2 are shown in Figs. 2-4 for $p$=40 (for indirect method, the number of states is selected to be 40). From these figures, it shows that both direct methods and indirect method isolate and identify the real-time failure of each shaker regardless of the working status of the other shaker.

As discussed in the theoretical part, if the number of independent sensors $q$ is greater than or equal to the number of independent actuators $r$, any integer $p$ greater than or equal to$n/(q-r+1)$ can be chosen. As discussed in Eq. (10), the error function will be zero if the input from examined actuator equals to the commanded input without measurement noise.

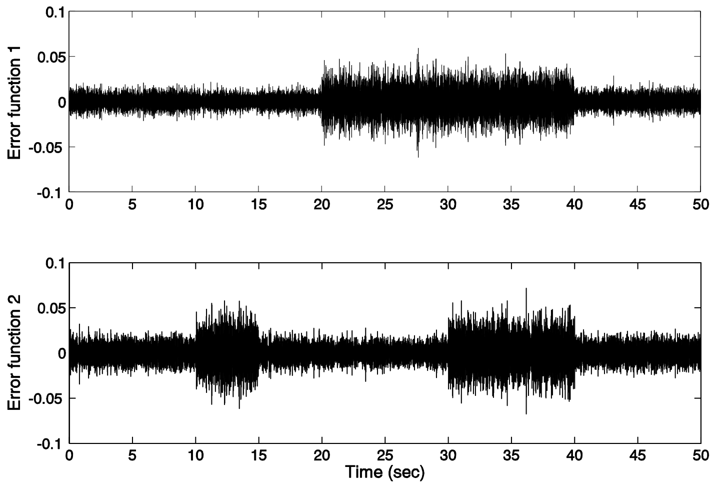


Fig. 2 Actuator error function from sensors 2 and 4's measurements using indirect method with $p$=40: (a) actuator 1, and (b) actuator 2

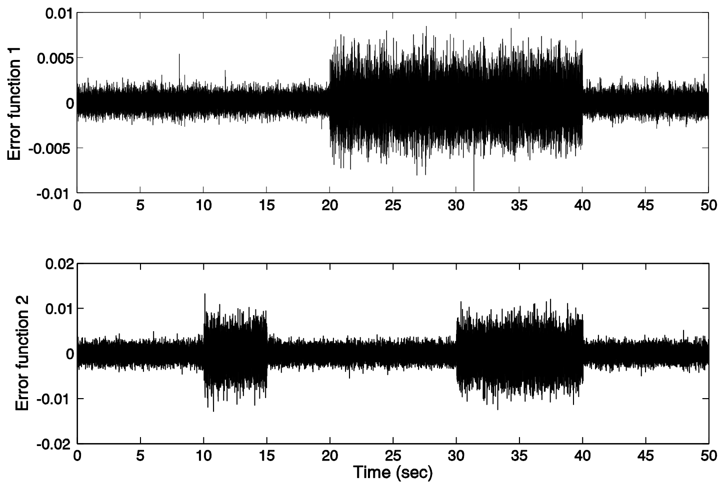


Fig. 3 Actuator error function from sensors 2 and 4's measurement using direct method 1 with $p$=40: (a) actuator 1, and (b) actuator 2

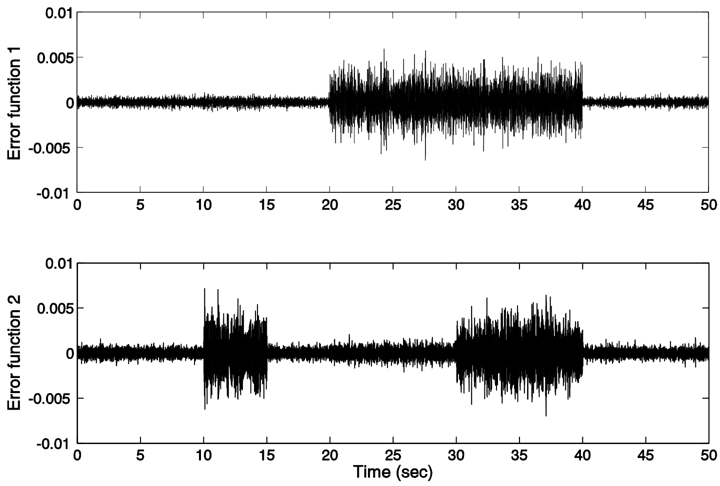


Fig. 4 Actuator error function from sensors 2 and 4's using direct method2 with *p*=40: (a) actuator 1, and (b) actuator 2

As shown in Figs. 2-4, due to the sensor measured noise, the error function shows non-zero values even the examined actuator work functionally. When the non-zero value profile due to sensor measured noise is greater than or equal to the non-zero value profile due to actuator failure, it is difficult to isolate and detect the failure of the examined actuator. To investigate the influence of different values of *p* on the error function, p=20, 40, 60, and 160 are selected. *l* is select to be 2000 to make the input-output long enough. The two parameters for different values of *p* are listed in Table 1. For the parameters shown in Table 1, the norm of coefficients $\mathrm{P}_i = [\beta_0^i,\ \beta_1^i,\ \cdots,\ \beta_{p-1}^i,\ \beta_p^i,\ \alpha_0^i,\ \alpha_1^i,\ \cdots,\ \alpha_{p-1}^i,\ \alpha_p^i]$ is kept to be one. As discussed in Eq. (20), even the norm of $\mathrm{P}_i$ is one, the coefficients of the error function are not unique. Instead, it is a subspace. Hence it is meaningless to directly compare the absolute value of the actuator failure error function. Instead, the ratio of the error function due to actuator failure and sensor measured noise are more meaningful for comparison. Two parameters: 1) the ratio (a in Table 1) between the maximal absolute values of the signal in the error function due to sensor measured noise and actuator failure; 2) the ratio (b in Table 1) between average absolute values of the signal in the error function due to sensor measured noise and actuator failure, are used for comparison. These values are shown in Table 1. From Table 1, it is observed that for each method, there exists a certain value of *p* in the error function that can maximally distinct the signal profile due to shaker failure from the signal profile due to sensor measured noise. For example, for the direct method, for the cases studied, the error signal profile due to shaker failure is most distinguishable when *p* equals to 60. While for direct method 2, when *p* equals to 40, the actuator failure is most distinguishable in the error function. But for indirect method, the signal profile due to shake failure can be maximally separated from measurement noise when *p* is 160.

Table 1 Parameters for the error function

| | | | *Indirect method* | | | *Direct method 1* | | | *Direct method 2* | | |
|---|---|---|---|---|---|---|---|---|---|---|---|
| | | | *Noise* | *Failure* | *Ratio* | *Noise* | *Failure* | *Ratio* | *Noise* | *Failure* | *Ratio* |
| $p$=20 | $e_1$ | a | 0.468 | 0.448 | 1.05 | 0.0156 | 0.0203 | 0.768 | 0.00457 | 0.0091 | 0.46 |
| | | b | 0.0785 | 0.0869 | 0.903 | 0.00179 | 0.00359 | 0.500 | 0.00104 | 0.0018 | 0.574 |
| | $e_2$ | a | 0.0437 | 0.0485 | 0.900 | 0.00702 | 0.0157 | 0.447 | 0.00327 | 0.0094 | 0.34 |
| | | b | 0.00759 | 0.00956 | 0.793 | 0.00123 | 0.00305 | 0.403 | 0.00061 | 0.0019 | 0.326 |
| $p$=40 | $e_1$ | a | 0.0286 | 0.0619 | 0.461 | 0.0054 | 0.0098 | 0.550 | 0.0011 | 0.0065 | 0.178 |
| | | b | 0.00472 | 0.011 | 0.428 | 0.00058 | 0.00177 | 0.327 | 0.00021 | 0.00123 | 0.174 |
| | $e_2$ | a | 0.0343 | 0.0716 | 0.480 | 0.0055 | 0.0132 | 0.414 | 0.0021 | 0.0072 | 0.296 |
| | | b | 0.0061 | 0.0128 | 0.473 | 0.00094 | 0.00257 | 0.363 | 0.00033 | 0.0015 | 0.217 |
| $p$=60 | $e_1$ | a | 0.211 | 0.416 | 0.508 | 0.0041 | 0.0064 | 0.633 | 0.00058 | 0.00259 | 0.226 |
| | | b | 0.0040 | 0.0078 | 0.510 | 0.00041 | 0.00123 | 0.33 | 0.00012 | 0.00050 | 0.24 |
| | $e_2$ | a | 0.324 | 0.573 | 0.565 | 0.00392 | 0.00957 | 0.41 | 0.00109 | 0.0034 | 0.32 |
| | | b | 0.0061 | 0.0120 | 0.504 | 0.00063 | 0.0018 | 0.34 | 0.00017 | 0.00062 | 0.272 |
| $p$=160 | $e_1$ | a | 0.0156 | 0.0711 | 0.219 | 0.0001 | 0.00036 | 0.284 | 0.00052 | 0.0185 | 0.283 |
| | | b | 0.0032 | 0.014 | 0.232 | 0.00016 | 0.00021 | 0.77 | 0.0007 | 0.00074 | 0.94 |
| | $e_2$ | a | 0.0183 | 0.0542 | 0.337 | 0.00035 | 0.00108 | 0.324 | 0.0031 | 0.0061 | 0.503 |
| | | b | 0.00368 | 0.0117 | 0.316 | 0.00046 | 0.00129 | 0.356 | 0.00363 | 0.00687 | 0.528 |

From the above experimental results, smaller value of $p$ is needed to obtain error function in which the signal profile due to actuator failure can be maximally separated from the sensor measured noise. This is because that the direct methods calculate the error function's coefficients directly from healthy input-output data and bypass the system identification step. For the system identification part, in order to match the output generated from the identified state-space matrices with the measured structural responses, the number of states need to be increased in the system realization step. From the theoretic part, the value of $p$ needs to be greater than or equal to $n/(q\text{-}r+1)$. So increasing the number of identified states will increase the minimal number $p$ to obtain the coefficients of the error function. However, in the meantime, it will brought more measurement noise influence into the error function.

The direct approaches, which bypass the intermediate system identification step, can avoid the unnecessary increasing number of states and reduce the influence of measurement noise to the error function.

To check the influence of different sensor locations on the error function, the pair of sensors are installed at different locations of the truss, as shown in Table 2. For location (a), the accelerometers are all collocated with both shakers; for location (b), accelerometers are all non-collocated with shakers; for location (c), there is a collocated shaker/accelerometer pair and the other accelerometer is not collocated with the other shaker. For location (c) case, the error functions have been shown in Figs. 3 and 4. For (a) and (b) cases, the error functions using both direct methods are shown in Figs. 5 to 8. From these figures, it is clear that the error functions are influenced by the sensor locations, but in this study, these influence are minor compared to the values of $p$.

The direct methods do not need the physical matrices of the test structure, such as mass, damping, and stiffness matrices. It even by pass the intermediate system identification step: the identification of the state-space matrices **A**, **B**, **C**, **D** by system identification method, such as OKID-ERA. The direct methods calculate the error function's coefficients directly from the healthy input-output data. Hence, the direct methods also bypass the errors incurring during the system identification process and minimize the influence of measurement noise in the error function.

Table 2 Three sensor sets: (a), (b), and (c) in Fig. 1

| Location set | Bay (sensor) number |
|---|---|
| (a) | Bay (5)(Sensor 1), Bay 1 (Sensor 4) |
| (b) | Bay (4)(Sensor 2), Bay 3 (Sensor 3) |
| (c) | Bay (4)(Sensor 2), Bay 1 (Sensor 4) |

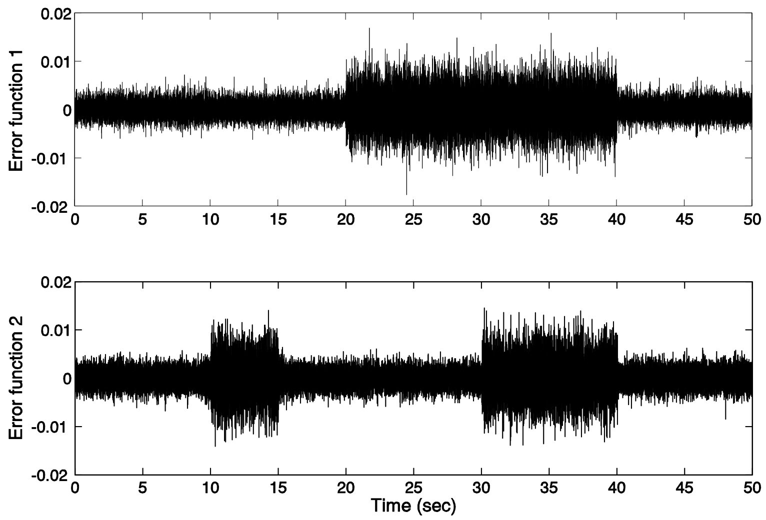


Fig. 5 Actuator error function from sensors 1 and 4's measurement using direct method 1 with $p$=40: (a) actuator 1, and (b) actuator 2

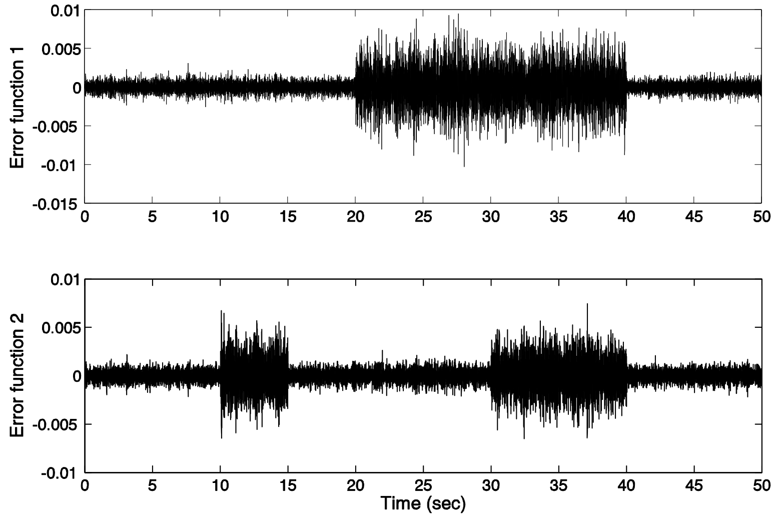


Fig. 6 Actuator error function from sensors 1 and 4's measurement using direct method 2 with $p$=40: (a) actuator 1, and (b) actuator 2

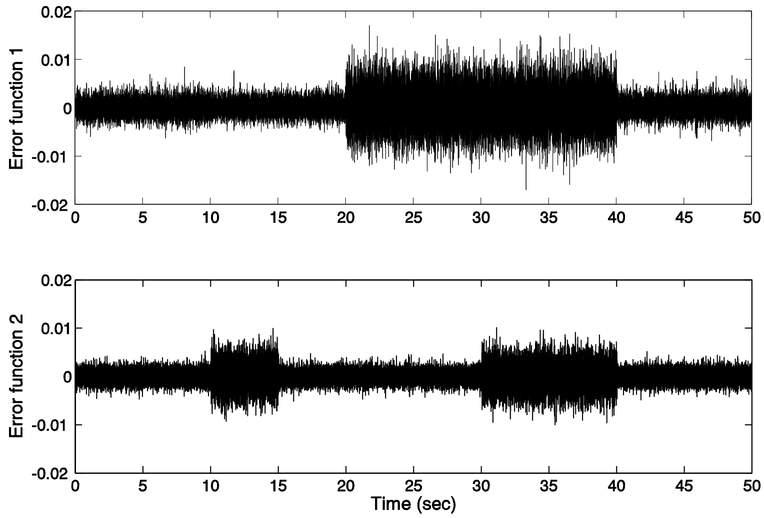


Fig. 7 Actuator error function from sensors 2 and 3'smeasurement using direct method 1 with $p$=40: (a) actuator 1, and (b) actuator 2

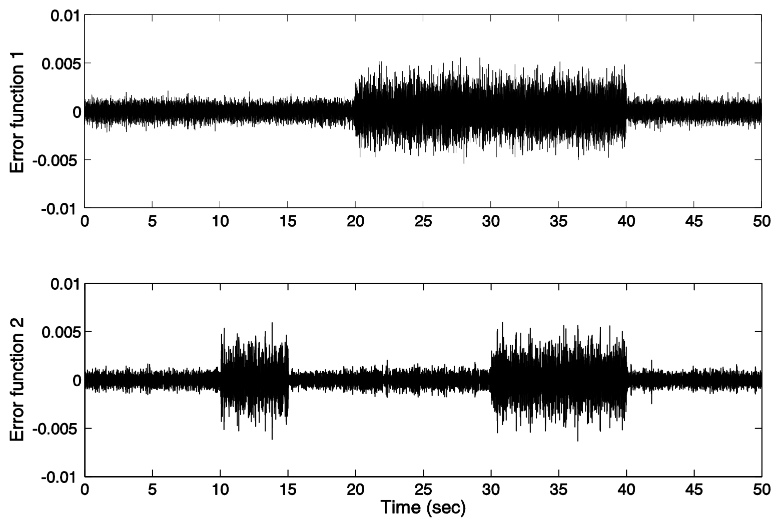


Fig. 8 Actuator error function from sensors 2 and 3's measurement using direct method 2 with $p$=40: (a) actuator 1, and (b) actuator 2

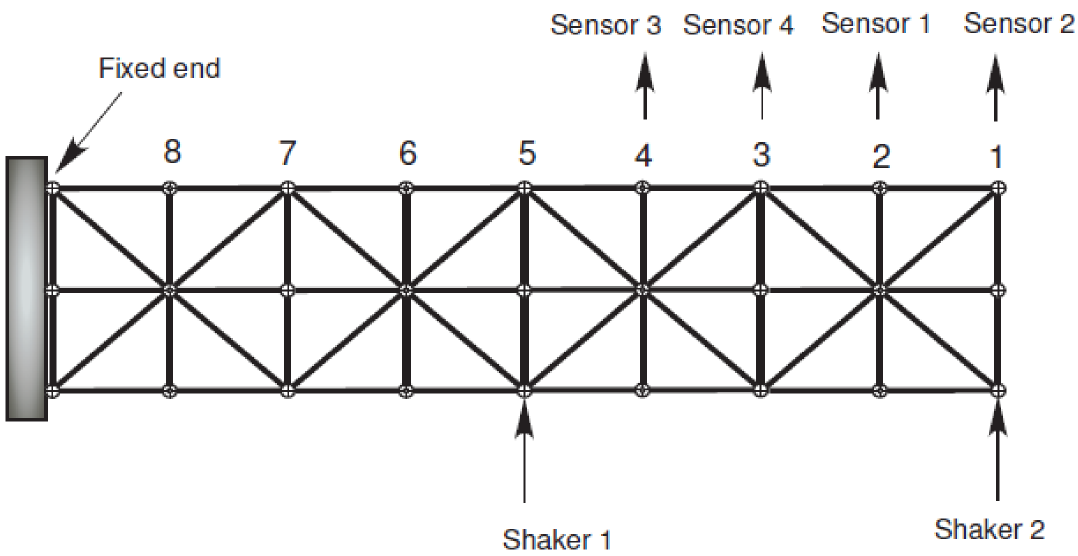


Fig. 9 Plan view of the schematic of the four meters long NASA eight bay truss structure

### 5.2 Experimental verification for direct sensor failure detection method

The same NASA 8-bay truss is used to verify the developed sensor failure algorithm. The plan view of the schematic of the eight-bay NASA truss is shown in Fig. 9. Two actuators are mounted on the 8-bay truss, one on the first bay and another one on the fifth bay. Four sensors are mounted from the first bay to the fourth bay. For this experiment, the total simulation time is 80 seconds and the sampling time is 0.001 seconds. The accelerometers mounted on the third and fourth bays are assumed to be the reference sensors that measure the correct structural response; these sensors are used to monitor the condition of the uncertain sensors mounted on the first and second bays.

In this experiment, the uncertain sensor mounted on the first bay (sensor 2) was disconnected from the signal conditioner during 30 to 40 seconds to simulate one type of sensor failure -- sensor totally fails to measure the structural response and produces zero measurement. Between 50-60 seconds, the amplitude of the output from uncertain sensor 2 was reduced by half using the built in function in the Simulink toolbox to simulate the amplitude reduction type of sensor failure. Uncertain sensor mounted on the second bay (sensor 1) was disconnected from the signal conditioner from 35 to 45 seconds and the amplitude of outputs was reduced by forty percent from 55 to 65 seconds. The first 1.5 seconds of the data, which is nearly 19 times of the fundamental period of the truss structure, were used to calculate each uncertain sensor's error function coefficients. The error function for uncertain sensor 1 and uncertain sensor 2 by direct methods for $p$=40 are shown from Figs. 10 and 11. From these figures, it is clear that the error functions using direct methods successfully detect and isolate the uncertain sensor's failure in real time. Due to the existence of measurement noise at the reference sensors, the error functions for uncertain sensors also show on-zero values even when the uncertain sensors do not fail.

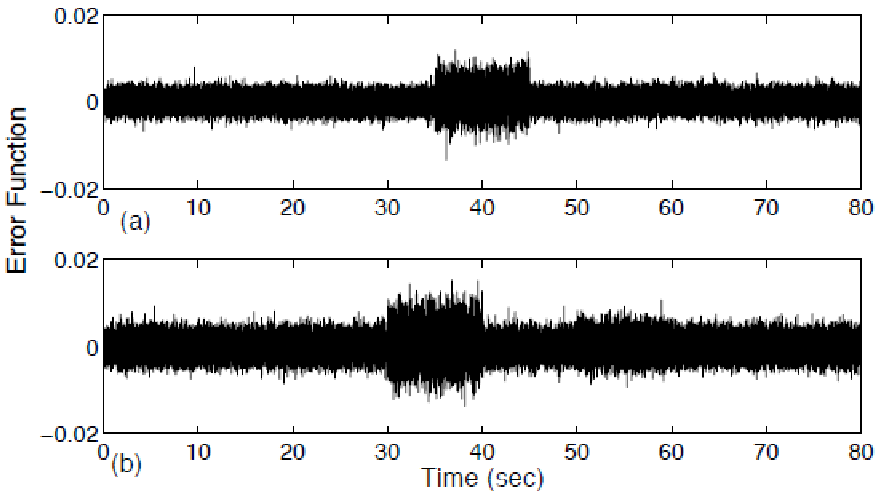


Fig. 10 Sensor error function for uncertain sensors 1 and 2 using direct method 1 with $p$=40: (a) uncertain sensor 1, and (b) uncertain sensor 2

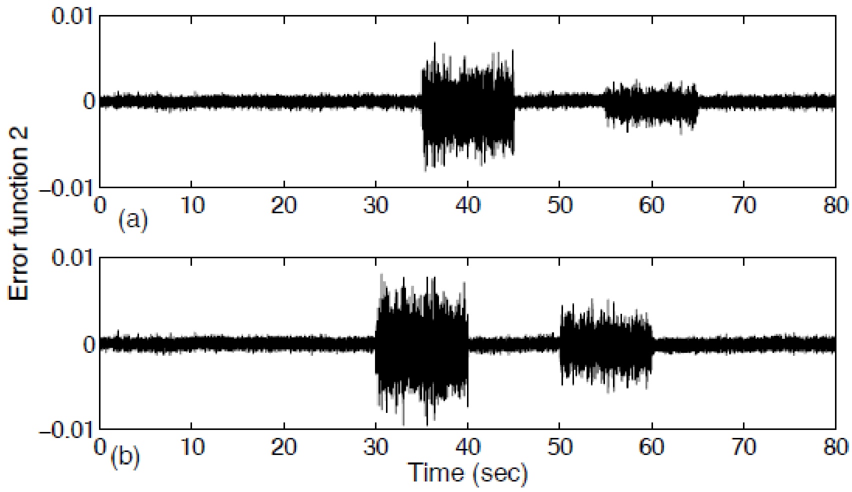


Fig. 11 Sensor error function for uncertain sensors 1 and 2 using direct method 2 with $p$=40: (a) uncertain sensor 1, and (b) uncertain sensor 2

## 6. Conclusions

The experimental studies demonstrate the performance of direct actuator failure detection algorithm. The actuator's error functions, which are directly calculated from the healthy data of the examined actuator and the all measured structure response, can real-time monitor the working status of the examined actuator. These direct methods bypass the intermediate system realization step and avoid the error incurring during such realization. Experimental results from the eight bays NASA truss show that the direct method can successfully isolate and real-time identify the failure of the two shakers attached to the structure. It has also been shown in the experiment that the error functions using direct method can distinct the non-zero signal due to actuator failure from non-zero value due to sensor measured noise with smaller number of p. Experimental results also verify that the direct sensor failure method can isolate and detect the uncertain sensor failures in real time without knowing the input information.

## References

Beard, R.V. (1971), *Failure accommodation in linear systems through self-reorganization*, Rep. MVT-71-1, Man-Vehicle Lab, MIT. Cambridge, MA.

Chen, J. and Patton, R.J. (1999), *Robust model-based fault diagnosis for dynamic systems*, Kluwer Academic publishers, Norwell, Massachusetts, USA.

Frank, P.M. (1990), “Fault diagnosis in dynamic systems using analytical and knowledge based redundancy-a survey and some new results”, *Automatica*, **26**(3), 459-474.

Gertler, J. (1991), “A survey of fault detection and identification methods”, *Proceeding of the IFAC, IMACS safe processes symposium*, Baden.

Gertler, J. and Dipierro, G. (1997), “On the relationship between parity relations and parameter estimation”, *Proceedings of the IFAC symposium on fault detection*, *supervision and safety for technical processes*: *SAFE PROCESS '97*, Pergamon 1998, Univ. of Hull, UK.

Gertler, J., Fang, X.W. and Luo, Q. (1990), *Detection and diagnosis of plant failures; the orthogonal parity equation approach*, (Ed. Leondes, C. ), Control and dynamics systems, 37, Academy Press.

Jones, H. L. (1973), *Failure detection in linear system*, MIT.

Koh, B.H., Li, Z., Dharap, P., Nagarajaiah, S. and Phan, M.Q. (2005), "Actuator failure detection through interaction matrix formulation", *J. Guid. Control Dynam.*, **28**(5), 895-901.

Li, Z., Koh, B.H. and Nagarajaiah, S. (2007), "Detecting sensor failure via decoupled error function and inverse input-output model", *J. Eng. Mech. - ASCE*, **133**(11), 1222-1228.

Massoumnia, M.A. (1986), "A geometric approach to the synthesis of failure detection filters", *IEEE T. Automat. Contr*., **31**(9), 839 - 846.

Spencer Jr., B.F. and Nagarajaiah, S. (2003), "State of the art of the structural control", *J. Struct. Control - ASCE*, **129**(7), 845-856.

Watanabe, K. and Hammelblau, D.M. (1982), "Instrument fault detection in systems with uncertainty", *Int. J. Syst. Sci.*, **13**(2), 137-158.

White, J.E. and Speyer, J.L. (1987), "Detection filter design: spectral theory and algorithms", *IEEE T. Automat. Control*, **32**(7), 593-603.

Wunnenberg, J. (1990), *Observer-based fault detection in dynamic systems*, Ph. D. thesis, Univ. of Duisburg, Germany.

Wunnenberg, J. and Frank, P.M. (1987), *Sensor fault using detection via robust observers*, (Eds., Tzafestas, S.G., Singh, M.G. and Schmidt, G.), *system fault diagnostics, reliability and related knowledge-based approaches*, D. Reidel Press, Dordrecht.